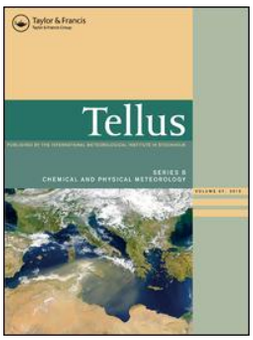

Tellus B: Chemical and Physical Meteorology

ISSN: (Print) 1600-0889 (Online) Journal homepage: https://www.tandfonline.com/loi/zelb20

The main controls of the precipitation stable isotopes at Kathmandu, Nepal

Niranjan Adhikari, Jing Gao, Tandong Yao, Yulong Yang & Di Dai

To cite this article: Niranjan Adhikari, Jing Gao, Tandong Yao, Yulong Yang & Di Dai (2020) The main controls of the precipitation stable isotopes at Kathmandu, Nepal, Tellus B: Chemical and Physical Meteorology, 72:1, 1-17, DOI: 10.1080/16000889.2020.1721967

To link to this article: https://doi.org/10.1080/16000889.2020.1721967

Published online: 10 Feb 2020.

Tellus SERIES B CHEMICAL AND PHYSICAL METEOROLOGY
PUBLISHED BY THE INTERNATIONAL METEOROLOGICAL INSTITUTE IN STOCKHOLM

The main controls of the precipitation stable isotopes at Kathmandu, Nepal

By NIRANJAN ADHIKARI[1,2], JING GAO[1,3]*, TANDONG YAO[1,3], YULONG YANG[1,2], and DI DAI[1,2], [1]*Key Laboratory of Tibetan Environment Changes and Land Surface Processes, Institute of Tibetan Plateau Research, Chinese Academy of Sciences, Beijing, China;* [2]*University of Chinese Academy of Sciences, Beijing, China;* [3]*CAS Center for Excellence in Tibetan Plateau Earth Sciences, CAS, Beijing, China*

(Manuscript Received 17 June 2019; in final form 16 December 2019)

ABSTRACT

Precipitation stable isotopes (^{2}H and ^{18}O) are adequately understood on their climate controls in the Tibetan Plateau, especially the north of Himalayas via about 30 years' studies. However, knowledge of controls on precipitation stable isotopes in Nepal (the south of Himalayas), is still far from sufficient. This study described the intra-seasonal and annual variations of precipitation stable isotopes at Kathmandu, Nepal from 10 May 2016 to 21 September 2018 and analysed the possible controls on precipitation stable isotopes. The enriched δD and $\delta^{18}O$ values were identified during non-monsoon season and depleted values were found during monsoon season, showing remarkable intra-seasonal characteristics of monsoon influence. The local meteoric water line suggested a strong influence of evaporation during rainfall in non-monsoon season and significant impact of non-equilibrium processes on precipitation during monsoon season. Temperature–$\delta^{18}O$ exhibited negative correlation for overall samples and showed no significant correlation in seasonal scales, which was attributed to the influence of monsoon moisture. The positive correlation was observed between $\delta^{18}O$ and outgoing longwave radiation (OLR) in monsoon season, suggesting the significant impact of convective activity on temporal variations of precipitation stable isotopes. During April, and May of 2016 and 2017, variation of precipitation stable isotopes are probably related with the mixing of multi-moisture combined with the westerlies transport. Our study suggested that the moisture transport processes are the main controls of precipitation stable isotopes at Kathmandu.

Keywords: stable isotopes, precipitation, Indian monsoon, westerlies, Kathmandu

1. Introduction

Stable isotopic compositions (oxygen (^{18}O) and hydrogen (^{2}H)) of precipitation can be applied as an important tracer to understand the atmospheric moisture origin, hydrological processes, and effects of evaporation and condensation history of air masses (Dansgaard, 1964; Gao et al., 2011; He and Richards, 2016) due to the observed influences of evaporation, condensation, precipitation, and temperature as well as moisture transport processes on precipitation stable isotopes (Araguás-Araguás et al., 1998; Yao et al., 1999; Yu et al., 2014; Ren et al., 2016). The control of precipitation amount on precipitation stable isotopes, termed as "amount effect" which is shown as the negative correlation between precipitation $\delta^{18}O$ and precipitation amount, is suggested conventionally in the monsoon rainfall (Lachniet and Patterson, 2002; Sánchez-Murillo et al., 2013). However, this correlation is not persistent at all monsoon regions (Breitenbach et al., 2010) due to changes of seasons, locations, and time scales of precipitation (Yu et al., 2008, Cai and Tian, 2016). Many recent studies have found the significant role of convective activities on controlling precipitation stable isotopes in monsoon regions rather than simply precipitation amount (Risi et al., 2008; Lekshmy et al., 2014; Chakraborty et al., 2016).

Since, 1961, the International Atomic Energy Agency (IAEA) and the World Meteorological Organization (WMO) have been continuously monitoring the environmental and geographical controls on precipitation stable isotopes through Global Network of Isotopes in

*Corresponding author. email: gaojing@itpcas.ac.cn

Citation: Tellus B: 2020, **72**, 1445379, https://doi.org/10.1080/16000889.2020.1721967

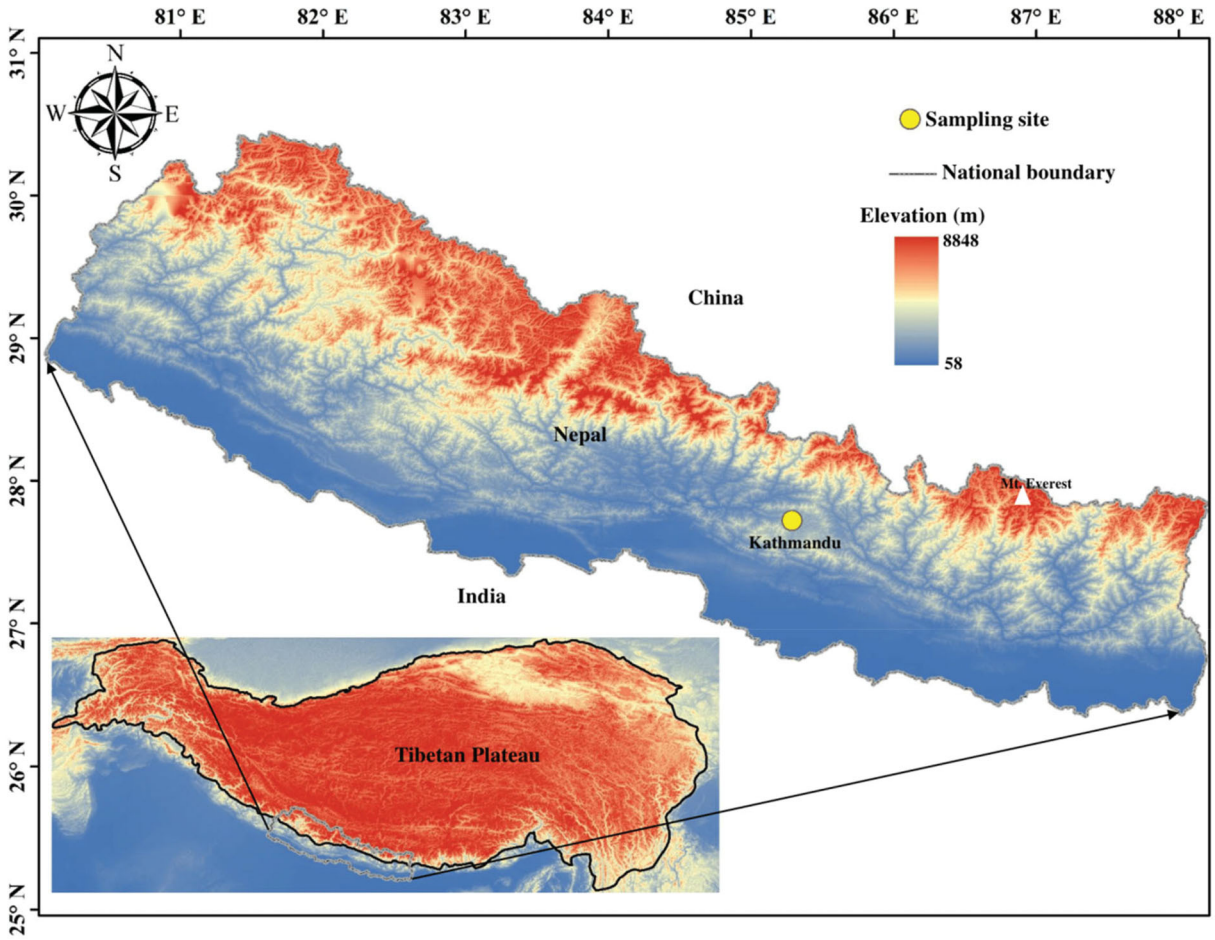

Fig. 1. Map showing the location of Kathmandu sampling site (yellow dot) on the south of Himalayas.

Precipitation (GNIP) project (Munksgaard et al., 2012; He et al., 2015; Ren et al., 2016). With the development of different monitoring network, many scientists began to take interest on stable isotopes studies and conducted various researches in different part of the globe. Earlier studies have demonstrated distinct "temperature effect", i.e. positive correlation between local temperature and precipitation $\delta^{18}O$, at the middle and high latitude regions (Pape et al., 2010; Chen et al., 2017) whereas precipitation amount effect is dominant in the tropical and monsoon regions (Lachniet and Patterson, 2002; Sánchez-Murillo et al., 2013). However, latest studies in the Asian monsoon region suggested that changes in moisture sources and/or their relative contributions are the main factors responsible for the seasonal variability on precipitation stable isotopes (Breitenbach et al., 2010).

Precipitation d-excess, defined as $d = \delta D - 8 \times \delta^{18}O$, (Dansgaard, 1964) has long been recognized as a diagnostic tool to provide the information of moisture sources, hydrological cycle, and local climate conditions (Tian et al., 2001; Liu et al., 2008). Precipitation d-excess, with a global average value of 10‰ reveals the kinetic isotopic fractionation in the moisture source region as a function of relative humidity, air temperature and wind speed at the source region and interaction or mixing of moisture along the water vapour trajectory (Rozanski et al., 1993; Clark and Fritz, 1997; Ren et al., 2017). Different scientific investigations and isotope models have revealed that the higher value of precipitation d-excess is associated with either precipitation derived from continental recycled moisture or due to lower condensation temperature and the lower d-excess value of precipitation is associated with either precipitation derived from maritime moisture or sub cloud evaporation under dry climate. (Froehlich et al., 2001; Peng et al., 2007; Pang et al., 2011; Bershaw et al., 2012; Salamalikis et al., 2016).

Much isotopic investigation on precipitation has been carried out in the Tibetan Plateau (TP) (the north of Himalayas) and obtained lots of valuables research progress (Yao et al., 1999; Tian et al., 2001; Yu et al., 2008; Yao et al., 2013). Over the TP and surrounding regions, the interaction between the westerlies and Indian

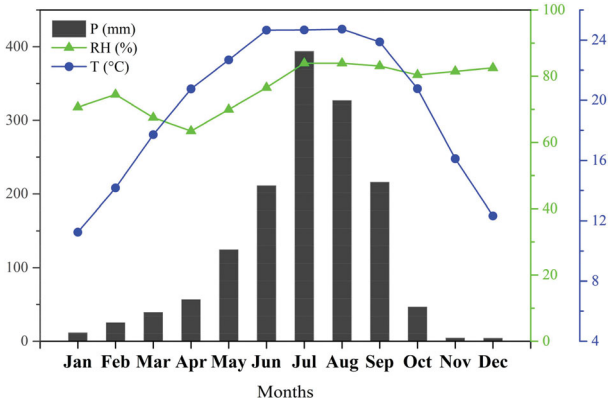

Fig. 2. Variation of monthly mean temperature (T), monthly sum of precipitation (P) and monthly average relative humidity (RH) at Kathmandu station from 2001 to 2018. Green line, blue line and grey bar represent relative humidity, temperature and precipitation, respectively.

monsoon are the main cause of large-scale spatial variation of precipitation stable isotopes. (Yao et al., 2013). Earlier studies found the distinct influence of different moisture transports on precipitation stable isotopes in the south-north transect of TP. The moisture transport in the northern TP is strongly dominated by the westerlies during the whole year, associated with the significant positive correlation between precipitation $\delta^{18}O$ and local temperature (Yao et al., 2013). Meanwhile, the depleted summer precipitation $\delta^{18}O$ in the southern TP is attributed to the moisture transport of Indian monsoon, showing negative correlation between $\delta^{18}O$ and precipitation amount at intra-seasonal scales. Due to multi-scale mixing between different moisture sources in the central TP, complicated $\delta^{18}O$ variations exist (Yao et al., 2013). However, in the southern slope of Himalayas, studies on precipitation stable isotopes are still far from sufficient.

Nepal, located in the south of Himalayas between the latitudes 26°22′N and 30°27′N and longitudes 80°04′E and 88°12′E, covers a great variety of altitude topography ranging from 60 m above sea level (asl) in the south to the height of Mount Everest (8848 m asl) in the north. Due to its complex topography, highly variable local weather can be felt over short geographical distances. The climate in Nepal is mainly controlled by two circulation system, summer monsoon circulation (mid-June to September) and the westerlies circulation (October to early June) (Shrestha et al., 2000). The summer monsoon is characterized by the south-easterly winds laden moisture coming from Bay of Bengal and the westerlies circulation is characterized by the westerlies winds laden moisture from Mediterranean Sea (Karki et al., 2016). Kathmandu, Nepal is an appropriate site to detect the alternating influence of the summer monsoon and the westerlies on variations of precipitation stable isotopes. Moreover, Kathmandu is situated at about the mid-point between Indo-Gangatic plain and Tibetan Plateau along the southern slope of Himalayas. So, the observed results reflect the mean scale isotopic variation from the south of Himalayas. Chhetri et al. (2014) conducted a preliminary study on precipitation stable isotopes at Kathmandu, which was mainly focused on the effect of surface air temperature and precipitation amount on precipitation stable isotopes. They reported that the depletion of precipitation $\delta^{18}O$ and δD during monsoon season (from mid-June to September) of the years 2011 and 2012 was mainly influenced by amount effect that was mainly linked with the intensive influence of Indian monsoon during that period. Then, the $\delta^{18}O$ and δD values increased after monsoon retreat and followed the temperature variation until summer monsoon onset, suggesting temperature effect and the enriched precipitation stable isotopes were related with the effect of the westerlies in dry season. Recent studies also suggested that variations in precipitation stable isotopes are also related to regional processes in the Asian monsoon region (Yang et al., 2011; Lekshmy et al., 2014; Chakraborty et al., 2016; Wei et al. 2018). However, we are not clear about the pronounced influence of regional processes or local meteorological condition on precipitation stable isotopes at Kathmandu at different time scales, especially during the transition period between the Indian monsoon and the westerlies.

The goal of this study is trying to understand the main control of precipitation stable isotopes at Kathmandu at different time scales and clarify the cause of variation of precipitation stable isotopes during the transition period between the Indian monsoon and the westerlies. We analysed the temporal variations (intra-seasonal and annual) of precipitation $\delta^{18}O$, δD and d-excess at Kathmandu from 10 May 2016 to 21 September 2018 with reference to local temperature and precipitation amount. We also detected the influence of moisture sources and transport paths as well as convective activities on precipitation stable isotopes by using reanalysis data and back trajectory analysis.

2. Sampling site, materials and methods

All the samples are located at Kathmandu (27°42′N, 85°20′E), the capital of Nepal, with an average elevation of about 1400 m above sea level (Fig. 1). Based on meteorological data from 1 January 2001 to 21 September 2018, the seasonal pattern of Precipitation (P), Temperature (T), and Relative Humidity (RH) is shown in Fig. 2. On the basis of this data, 78.56% of annual precipitation occurred in monsoon season (June to

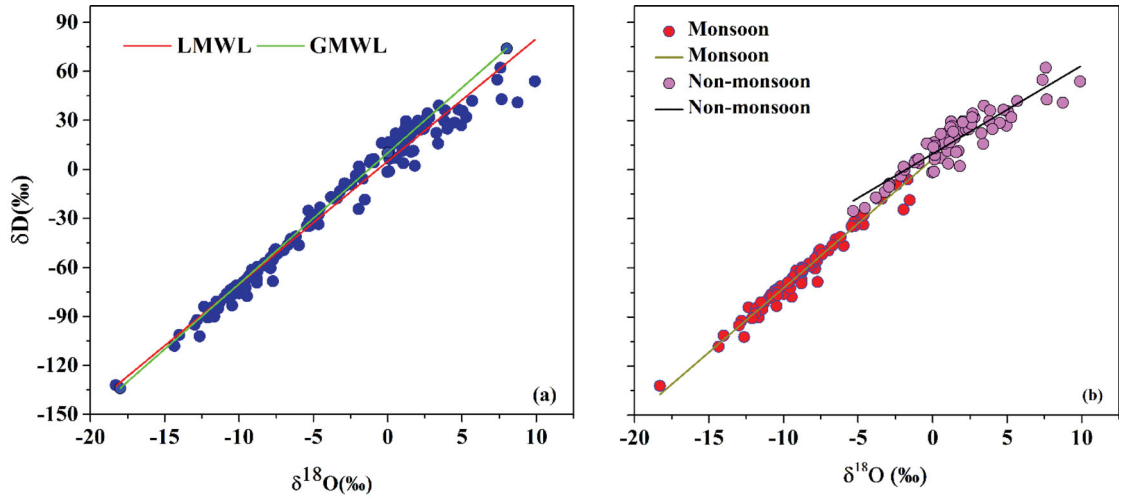

Fig. 3. Relationship between $\delta^{18}O$ and δD values of (a) overall precipitation and (b) monsoon and non-monsoon precipitation at Kathmandu.

September). Precipitation during pre-monsoon (MAM), post monsoon (ON) and winter season (DJF) has contributed to 15.11%, 3.51% and 2.81%, respectively. The monsoon season had an average temperature of 24.48 °C, followed by pre-monsoon (20.48 °C), post monsoon (18.44 °C) and winter season (12.58 °C). Similarly, the average relative humidity in monsoon season was 81.85%, followed by post monsoon (80.92%), winter (75.87%) and pre-monsoon season (66.95%).

The moisture in our study site is mainly affected by two circulation systems, Indian monsoon system (mid-June to September) and westerly circulation (October to May) (Karki et al., 2016). During monsoon season, the mixing of south westerlies originates from Arabian Sea and south easterlies originates from Bay of Bengal (BoB) transport warm–moist air mass to the study site and bring abundant precipitation. After the retreat of monsoon, the westerlies dominate the study site with pronounce decrease in air temperature and humidity in the region)

The Kathmandu Centre for Research and Education (KCRE) of Chinese Academy of Sciences and Tribhuvan University, Nepal collected precipitation samples at Kathmandu, Nepal. A total of 142 event-based precipitation samples from 10 May 2016 to 21 September 2018 were collected at KCRE. Rainfall from each precipitation event was collected and immediately stored in sealed polyethylene bottles with no air headspace to minimize the post-sampling isotopic fractionation. All the samples were then stored in refrigerator until analysis.

Precipitation $\delta^{18}O$ and δD of samples were measured by cavity ring down laser spectroscopy (CRDS, L2130-i Picarro water isotope analyser) in the Key Laboratory of Tibetan Environment Change and Land Surface Processes, Chinese Academy of Sciences. Analytical precision is typically 0.1‰ for $\delta^{18}O$ and 0.5‰ for δD based on long-term analysis of internal laboratory standards. All the measured data were calibrated and reported as relative to Vienna Standard Mean Ocean Water (V-SMOW), where $\delta(‰) = (R/R_{v\text{-}smow} - 1)\times 1000$ and R and $R_{v\text{-}smow}$ represent either the O^{18}/O^{16} or D/H ratios of the sample and standard, respectively. The weighted monthly average values of $\delta^{18}O$ and δD against precipitation amount were calculated by using the equation below.

$$\delta_{wt} = \frac{\sum P_i \times \delta^{18}O_i \ (or\ \delta D_i)}{\sum P_i} \quad (1)$$

where P_i and $\delta^{18}O_i$ $(or\ \delta D_i)$ denote the precipitation amount and corresponding isotopic values, respectively.

Daily air temperature, relative humidity and precipitation amount during each precipitation event were obtained from Khumaltar meteorological station, about 4 km away (aerial distance) from sampling site, monitored by the Department of Hydrology and Meteorology (DHM), Nepal.

Winds, specific humidity and outgoing longwave radiation over the study area from NCEP/NCAR reanalysis I datasets with a spatial precision of 2.5° for longitude-latitude grids were used in this study. (Available at https://www.esrl.noaa.gov/psd/) (Kalnay et al., 1996). TRMM daily rainfall data at each grid point extending from latitude 10°N to 50°N and from longitude 50°E to 100°E were also used to analyse the spatial correlation between precipitation amount and precipitation $\delta^{18}O$.

2.1. Back-trajectories

The Hybrid Single-Particle Lagrangian Integrated Trajectory Model (HYSPLIT, available from the NOAA Air Resources

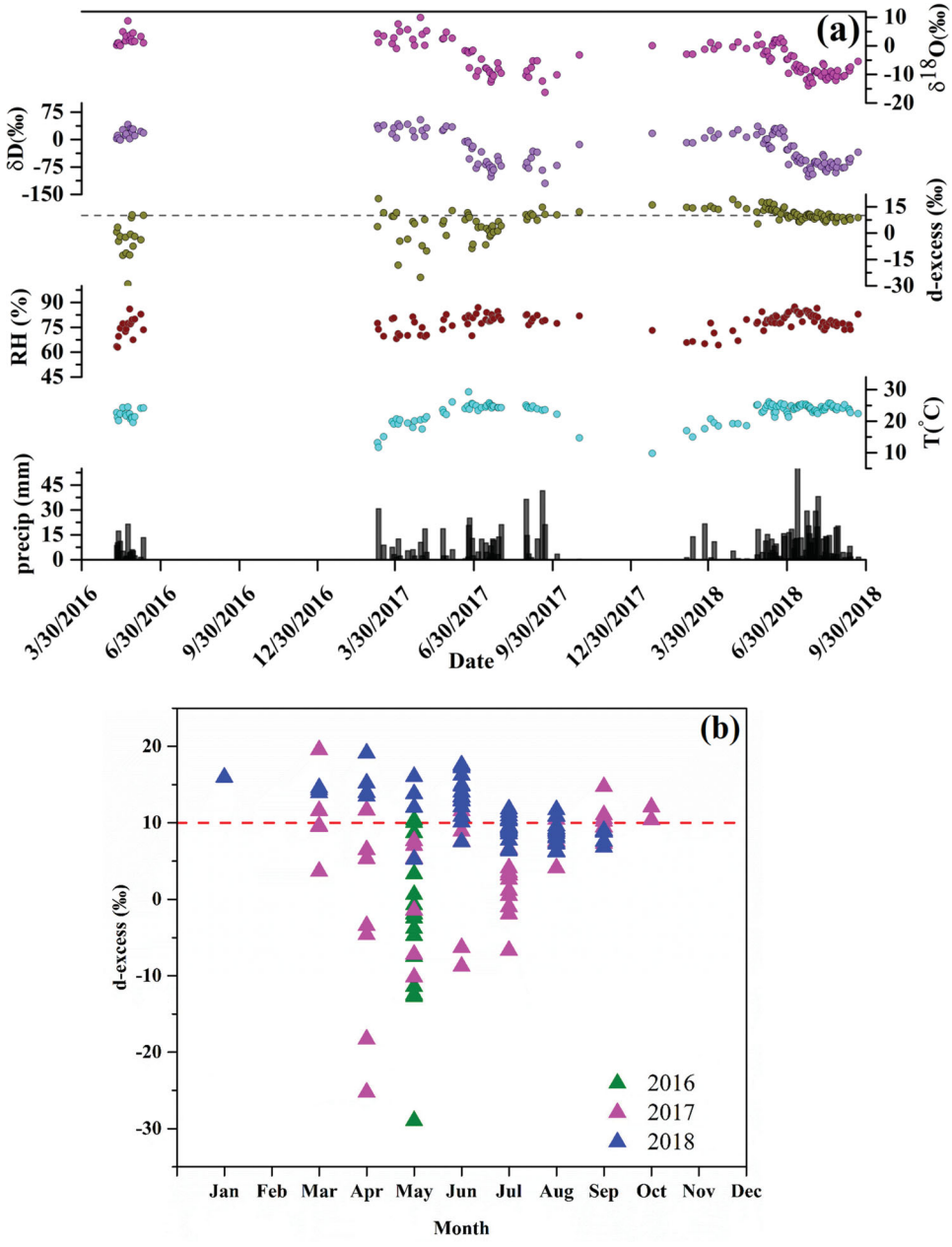

Fig. 4. (a) Temporal variations in precipitation amount, temperature, relative humidity, d-excess, δD, and $\delta^{18}O$ from 10 May 2016 to 21 September 2018 in Kathmandu. (b) Seasonal changes in d-excess at Kathmandu from 2016 to 2018. The green, pink, and blue triangles indicate the precipitation d-excess values in 2016, 2017 and 2018, respectively. The horizontal dashed line represents the global average of 10‰.

Laboratory at https://ready.arl.noaa.gov/HYSPLIT.php.) was used to calculate the backward trajectory of the air parcels for the precipitation events (Draxler and Hess, 1998). This model has been used together with precipitation stable isotopes to probe moisture sources and transport paths (Xie et al., 2011; Wu et al., 2015). The data set of Global Data Assimilation System (GDAS0P5, ftp://arlftp.arlhq.noaa.gov/pub/archives/gdas0p5) (Kleist et al., 2009) with spatial resolution of 0.5° was used as the meteorological data to run HYSPLIT model. In this study, backward trajectories of 120 h (5d) were performed for selected precipitation events. Considering the mean-state precipitation, we calculated back trajectories at 12-h time steps for three different altitudes (500 m, 1000 m, and 1500 m above ground level).

Table 1. Annual variation range of daily averaged $\delta^{18}O$, δD and d-excess (d) during the study period.

	2016			2017			2018		
	Min	Avg	Max	Min	Avg	Max	Min	Avg	Max
$\delta^{18}O$(‰)	0.09	2.55	8.74	−16.33	− 3.47	9.90	− 14.02	− 5.56	3.86
δD(‰)	− 1.22	16.96	40.94	− 120.07	− 23.81	53.93	− 101.26	− 33.51	36.12
d(‰)	− 28.97	− 3.47	10.36	− 25.25	3.95	19.54	5.25	10.96	19.13

Table 2. Summary of precipitation stable isotopes data along with temperature and precipitation amount between earlier study and present study at Kathmandu.

Observation period	Previous study 15 Feb 2011 to 22 July 2012	Recent study May 10 2016 to 21 Sept 2018
Number of samples	148	142
Overall mean $\delta^{18}O$(‰)	−3.91	−3.76
Overall mean δD(‰)	−27.29	−23.39
Overall mean d-excess(‰)	4.02	6.73
Mean air temperature(°C)	18.80	19.30
Annual average precipitation(mm)	1438	1023.93

3. Results and discussion

3.1. Relationship between $\delta^{18}O$ and δD

The linear relationship between $\delta^{18}O$ and δD derived from precipitation samples collected from one or more local sites relative to the global meteoric water line (GMWL, $\delta D = 8\times\ \delta^{18}O + 10$) (Craig, 1961) is defined as local meteoric water line (LMWL). The Local Meteoric Line (LMWL) depends on the climatic conditions of the region such as moisture source, condensation temperature and sub cloud evaporation. The slopes and intercepts of LMWL greater than GMWL represent precipitation with low temperature and low absolute moisture content of the air (Pang et al., 2011) whereas lower slopes and intercepts of LMWL as compared with GMWL indicate the effect of sub-cloud evaporation due to different non-equilibrium fractionation of oxygen and hydrogen (Dansgaard, 1964; Rozanski et al., 1993; Ren et al., 2017). The correlation between event-based $\delta^{18}O$ and δD values based on 142 precipitation samples collected from Kathmandu (defined here as local meteoric water line) is shown in Fig. 3a. The LMWL is defined by an equation:

$$\delta D = 7.52\pm0.11 \times \delta^{18}O + 4.92\pm0.76, (R^2 = 0.97, n = 142) \quad (2)$$

Chhetri et al. (2014) reported the LMWL of Kathmandu, which is defined as:

$$\delta D = \ 7.77 \times \delta^{18}O \ + 3.10, (R^2 = 0.96, \ n \ = \ 148) \quad (3)$$

The slope for our samples is smaller than that in Chhetri's study, and the larger intercept appears in our study. This indicates that precipitation during our sampling period suffered significant evaporative enrichment during rainfall as compared with Chhetri's study. But both LMWLs show lower slopes and smaller intercepts compared with GMWL, suggesting re-evaporation of raindrops at Kathmandu. We also separated the rainfall samples between non-monsoon and monsoon seasons and calculated the LMWL for different seasons (Fig. 3b). The LMWL in non-monsoon season defined by Equation (4), show significantly lower slope than GMWL indicating a strong influence of evaporation during that period.

$$\delta D = 5.39\pm0.29 \times \delta^{18}O + 9.66\pm0.99(R^2 = 0.84, n = 67) \quad (4)$$

The LMWL in the monsoon season is defined as,

$$\delta D = 7.85\pm0.15 \times \delta^{18}O + 6.36\pm1.39(R^2 = 0.97, n = 75) \quad (5)$$

In this case, the slope approaches to GMWL indicating limited impacts of non-equilibrium processes on precipitation samples at Kathmandu during that period. The significantly lower intercept in monsoon season reflects the high relative humidity at primary moisture sources at Kathmandu (Gao et al., 2011).

3.2. Temporal variations of stable isotopes in precipitation

The temporal variations of precipitation stable isotopes at Kathmandu, together with the corresponding observed precipitation amount, temperature and relative humidity, are presented in Fig. 4a. It is clear that there is a strong linear correlation between $\delta^{18}O$ and δD (R^2=0.97) for the

measured samples (Fig. 3a). Therefore, the precipitation $\delta^{18}O$ can be sufficient to interpret the temporal variations in precipitation.

The annual variation range of precipitation stable isotopes at Kathmandu is shown in Table 1. In May 2016, daily averaged $\delta^{18}O$ in precipitation varied from 0.09‰ to 8.74‰ with an average of 2.55‰ and δD varied from −1.22‰ to 40.94‰ with an average of 16.96‰. In 2017, $\delta^{18}O$ and δD show large variability and lower averages compared to that in 2016. In 2018, precipitation stable isotopes ranged from −14.02‰ to 3.86‰ for $\delta^{18}O$, with an average of −5.56‰ and from −101.26‰ to 36.12‰ for δD, with an average of −33.51‰, showing narrower ranges than in 2017. Comparing our recent data with previous study (Table 2), annual averages of precipitation stable isotopes during our study period showed slightly higher than previous study. The mean air temperature/precipitation during overall sampling period is higher/lower compared with that of previous study.

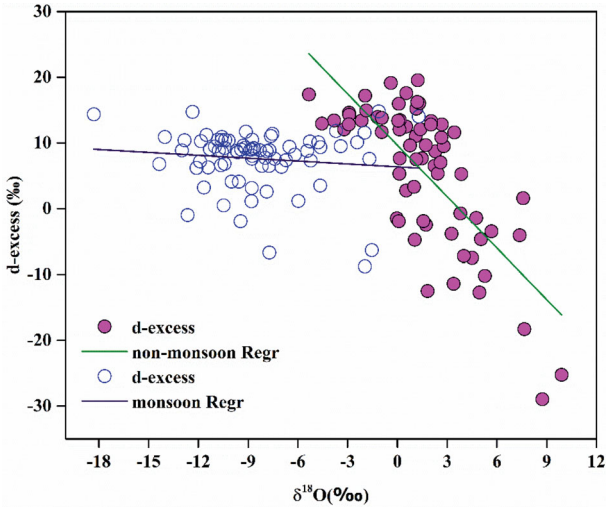

Fig. 5. Relationship between d-excess and $\delta^{18}O$ in precipitation events during monsoon and non-monsoon season.

Precipitation displays generally low $\delta^{18}O$ in the monsoon season (mid-June to September) and high values in the non-monsoon season (October to early June). The minimum value was recorded on 21 September 2017 (monsoon) and maximum value was on 29 April 2017 (pre-monsoon). The obvious variation ranges of $\delta^{18}O$ in 2016, 2017 and 2018 may signify different control factors on the annual timescale.

3.3. Deuterium excess

The conspicuous annual differences of d-excess are shown from 2016 to 2018 (Table 1). Although, the precipitation samples were collected in pre-monsoon season only in 2016, the d-excess showed large variation from −28.97‰ to 10.36‰ with average of −3.47‰. The d-excess values showed narrower ranges in 2018 as compared to former years (Table1). The minimum value (−28.97‰) was observed on 23 May 2016 and maximum value (19.54‰) was observed on 11 March 2017 during entire sampling period. d-excess decreases gradually from mid-June to end of September due to the development of Indian monsoon (Yao et al., 2013). More depletion of d-excess from March to June appeared in 2016 and 2017 compared with that in 2018 and most of the precipitation events occurred in April and May with lower d-excess values than the global average (10‰) (Fig. 4b). The year-round enriched d-excess in 2018 appeared. These annual differences may result from the different moisture sources and transport paths. We'll discuss in details in section 3.5.

Table 4. Precipitation samples showing high $\delta^{18}O$ and δD at the time of relatively high precipitation amount.

Date	$\delta^{18}O$	δD	d-excess	Precipitation
23 May, 2016	8.74‰	40.94‰	- 28.97‰	21.5mm
25 May, 2017	2.43‰	24.82‰	5.34‰	18.80mm
27 May, 2018	3.86‰	36.12‰	5.25‰	18.40mm

Table 3. Correlations of $\delta^{18}O$ and d-excess with temperature (T), precipitation (P), relative humidity (RH), and vapour pressure deficit (VPD) at different timescales. The number in parentheses indicates sample size.

Timescale		Overall sampling period		Mid-June to September		October to early June	
		$\delta^{18}O$	d-excess	$\delta^{18}O$	d-excess	$\delta^{18}O$	d-excess
Event	T	−0.44 (135)***	−0.03(135)	0.16(73)	−0.22(73)*	0.02(62)	−0.09(62)
	P	−0.25(135)**	0.08(135)	−0.19(73)	0.26(73)*	0.06(62)	−0.07(62)
	RH	−0.4(135)***	0.14(135)	−0.002(73)	0.16(73)	−0.01(62)	0.08(62)
	VPD	0.06 (135)	−0.18(135)*	0.07(73)	−0.23(73)*	−0.001(62)	−0.16(62)
Monthly	T	−0.42(17)	−0.22(17)	0.25(9)	−0.71(9)*	0.39(8)	−0.60(8)
	P	−0.27(17)	−0.02(17)	−0.20(9)	0.24(9)	0.55(8)	−0.56(8)

Note: ***, **, * indicate significant correlation at level .001, .01, and .05, respectively.

Table 5. Values of weighted $\delta^{18}O$, weighted d-excess and δD- $\delta^{18}O$ correlation parameters (slope, intercept and R^2) for different amount (mm) intervals in precipitation collected at Kathmandu from 10 May 2016 to 21 Sept 2018.

Samples		N	P	$\delta^{18}O$	d-excess	Slope	δD-$\delta^{18}O$ Intercept	R^2
All	135	135	1241.8	−5.32	7.58	7.52	4.86	0.97
$p \geq 25$	all	8	289.6	−8.68	11.93	8.56	16.65	0.99
	Monsoon	7	258.8	−9.86	11.02	7.23	3.14	0.99
$5 \leq p < 25$	all	63	809.79	−4.36	6.05	7.41	3.82	0.97
	Monsoon	34	481.8	−8.47	7.67	8.05	7.82	0.98
	Non-monsoon	29	327.99	1.66	3.68	4.85	9.89	0.84
$p < 5$	all	64	142.41	−3.90	5.70	7.65	5.57	0.97
	Monsoon	32	76.39	−8.72	6.89	7.79	5.29	0.96
	Non-monsoon	32	66.02	1.67	4.31	5.72	9.20	0.83

Figure 5 showed the linear correlation between $\delta^{18}O$ and d-excess. $\delta^{18}O$ is significantly anti-correlated with d-excess in non-monsoon season (R^2=0.55, $p < .001$, $n = 67$), but does not show significant correlation in monsoon season (R^2=0.01, $p > .34$, $n = 75$). This may indicate the effect of sub cloud evaporation on precipitation stable isotopes in non-monsoon season that was also demonstrated by previous studies (Froehlich et al., 2001; Tian et al., 2001; Ren et al., 2017). Out of 135 precipitation events (daily averaged) we collected, 64 precipitation events occurred with amount less than 5 mm and out of which 54 precipitation events occurred with surface air temperature higher than 20 °C suggested a favourable condition for sub-cloud evaporation (Crawford et al., 2017). The rainfall on 18 and 21 September 2017 showed extremely low $\delta^{18}O$ with relatively high d-excess that might be associated with the heavy convective rainfall (He and Richards, 2016).

3.4. Relationship between precipitation stable isotopes ($\delta^{18}O$and d-excess) and local climates

In order to identify the relationships between precipitation stable isotopes ($\delta^{18}O$ and d-excess) and local climates, we calculated the correlations among precipitation stable isotopes and corresponding air temperature, precipitation, relative humidity and vapour pressure deficit at daily and monthly scales. The correlation coefficients with their respective p values are shown in Table 3. There is significantly negative correlation between daily averaged $\delta^{18}O$ and temperature during our study period, opposite to temperature effect (Dansgaard, 1964; Rozanski et al; 1992). However, except a significant negative/positive correlation between d-excess and temperature/precipitation amount in monsoon season, no significant correlation was found between temperature and precipitation stable isotopes during monsoon and non-monsoon season at daily scales, separately (Table 3). It is noticed that all the significant correlations are disappeared at monthly scales during our study period. This finding contradicts with the result of Chhetri et al. (2014) which found a significant temperature effect for event based precipitation during dry season at Kathmandu. Although, some studies (e.g. Chhetri et al., 2014; Yu et al., 2015) have pointed out that temperature effect was found during their observation period when the southern branch of the westerlies was the sole moisture source for precipitation at Kathmandu in the dry season, we suggested that the influence of temperature on precipitation stable isotopes acts beyond the moisture transport processes at Kathmandu.

A significantly negative correlation was observed between daily averaged $\delta^{18}O$ and RH during the overall sampling period (Table 3), and the negative correlation between d-excess and vapour pressure deficit (VPD) that was defined as the difference between saturated vapour pressure and actual vapour pressure reflecting the evaporation between raindrops and atmosphere (Wu et al., 2015) was found. In addition, $\delta^{18}O$ showed a negative relationship with precipitation amount at daily scale during the overall period but no significant correlation was found at monthly or seasonal scales. Precipitation events on 23 May 2016, 25 May 2017 and 27 May 2018 showed much high $\delta^{18}O$ and δD values compared with other events with similar precipitation amounts (Table 4), which is opposite to amount effect (Dansgaard, 1964; Yu et al., 2014; Wu et al., 2015; Ren et al., 2017). These results confirmed the hypnosis effect of moisture transport processes we suggested above.

Considering the precipitation (P) intensity, observed precipitation events were sub-divided into three groups ($P \geq 25$mm, $5\,mm \leq P < 25$mm and $P < 5$mm) (Table 5). The averaged d-excess were decreasing with the decreasing of P. Meanwhile $\delta^{18}O$ was increasing. The rainfall events with $P \geq 25$mm displayed the highest slope and intercept of the linear regression between δD and $\delta^{18}O$

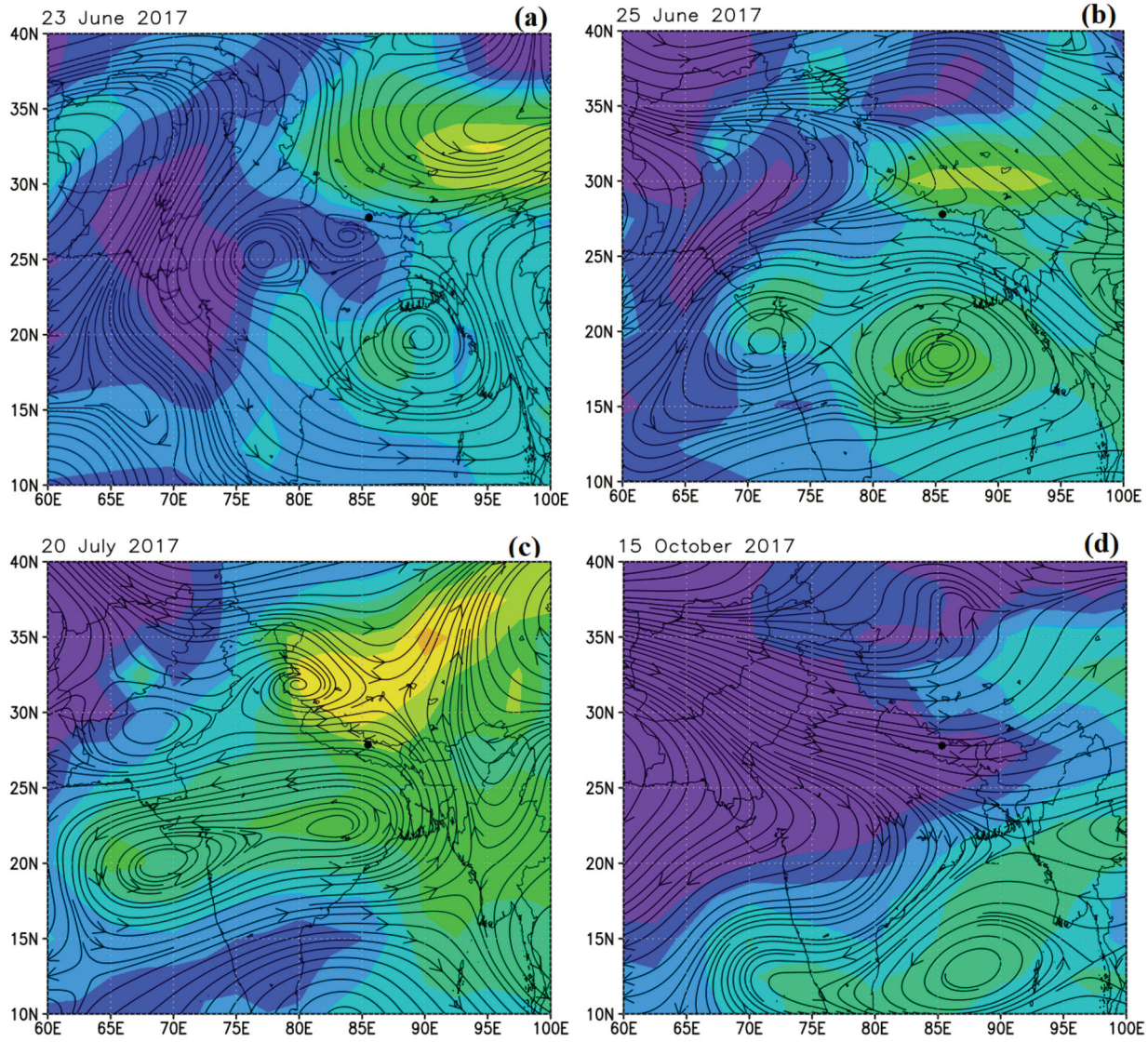

Fig. 6. Distributions of wind and specific humidity field over Kathmandu (black dot) and its adjacent regions at 500 hPa on (a) 23 June 2017, (b) 25 June 2017, (c) 20 July 2017, (d) 15 October 2017, (e) 6 May 2018, (f) 23 June 2018, and (g) 27 June 2018. The arrows indicate wind vectors, and the colour scale indicates specific humidity (g/kg).

among the three groups, and the weighted averaged d-excess with $P \geq 25$mm was slightly larger (11.93 ‰) than the global averaged value (10‰). Generally, most of these rainfall events with $P \geq 25$mm occurred in monsoon season with the moisture originated from Indian Ocean (Chhetri et al., 2014; Yu et al., 2015). However, we found one event that occurred on 11 March 2017 displayed high δD, $\delta^{18}O$ and d-excess (δD = 29.40‰, $\delta^{18}O = 1.23$‰ and d-excess = 19.54‰) with the moisture transported by the westerlies. This indicated the significant influence of moisture sources on precipitation stable isotopes rather than precipitation amount.

When precipitation amount distributed among $5\,mm \leq P < 25$mm and $P < 5$mm, δD-$\delta^{18}O$ regressions displayed slightly lower slopes (7.41 and 7.65, respectively) than GMWL and significantly lower intercept (3.82 and 5.57, respectively). When precipitation events were separated by monsoon and non-monsoon seasons, slopes of δD-$\delta^{18}O$ regression lines in monsoon season were approached to the slope of GMWL (8). These results further confirmed the limited impact of non-equilibrium processes in monsoon precipitation even. The lower intercepts in monsoon events might indicate the influence of oceanic moisture sources (Gao et al., 2011). In contrast,

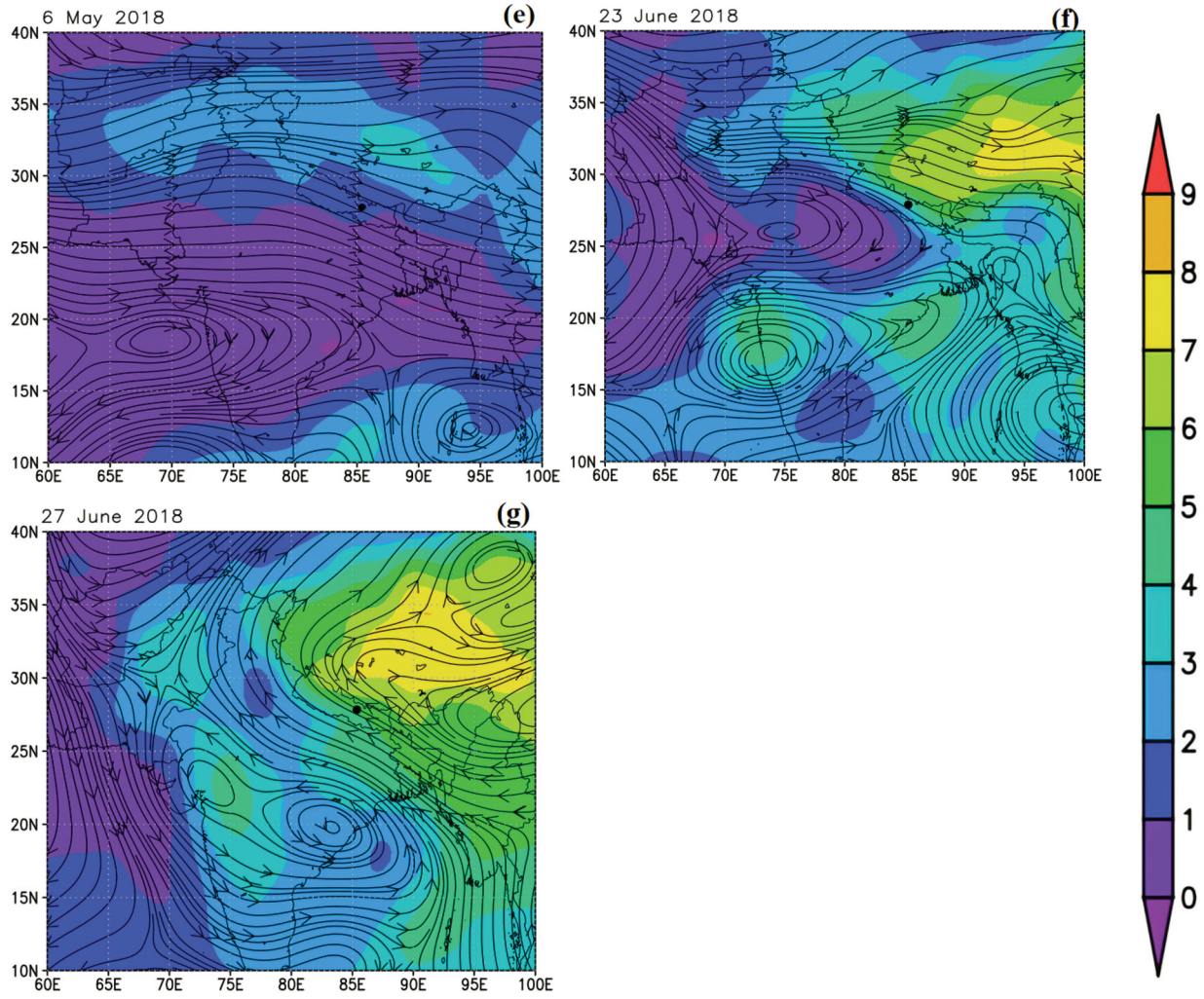

Fig. 6. (Continued)

slopes of δD-δ^{18}O regression lines in non-monsoon season were lower than 8. This emphasized the influence of re-evaporation on precipitation stable isotopes in non-monsoon season.

3.5. Moisture transport processes

To probe the influence of moisture transport processes on precipitation stable isotopes at Kathmandu, the daily winds pattern and the daily averaged specific humidity at 500 hPa over the study area were analysed on selected days in 2017 and 2018 (Fig. 6). On 23 June 2017, the study area was dominated by the westerlies with low specific humidity and averaged precipitation δ^{18}O of −1.98‰ (Fig. 6a). On 25 June 2017, the dominant moisture transport was changed to Indian monsoon with high specific humidity (Fig. 6b) and more depleted precipitation δ^{18}O (−7.71‰). The peak of δ^{18}O values on 23 June (2.65‰) depleted suddenly on 27 June 2018 (−1.12‰) (Figs. 6f and 6g). The sharp depletion of precipitation stable isotopes at the preliminary stage of monsoon may indicate the change of moisture sources transported by Indian monsoon. With the maturing of the summer Indian monsoon associated with high specific humidity (Fig. 6c) and heavy precipitation (Fig. 4), the moisture source and intensity of precipitation were varying. The progressive depletion of precipitation δ^{18}O from mid-June to end of September is mainly related to the influence of Indian monsoon. As marine air masses moves towards the continent, deep convection and cyclonic activity occurred over the Indian Ocean and the orographic rise leads to adiabatic cooling of northward moving air masses which causes heavy rainfall at Kathmandu (Tian et al., 2001; Yu et al., 2015). However,

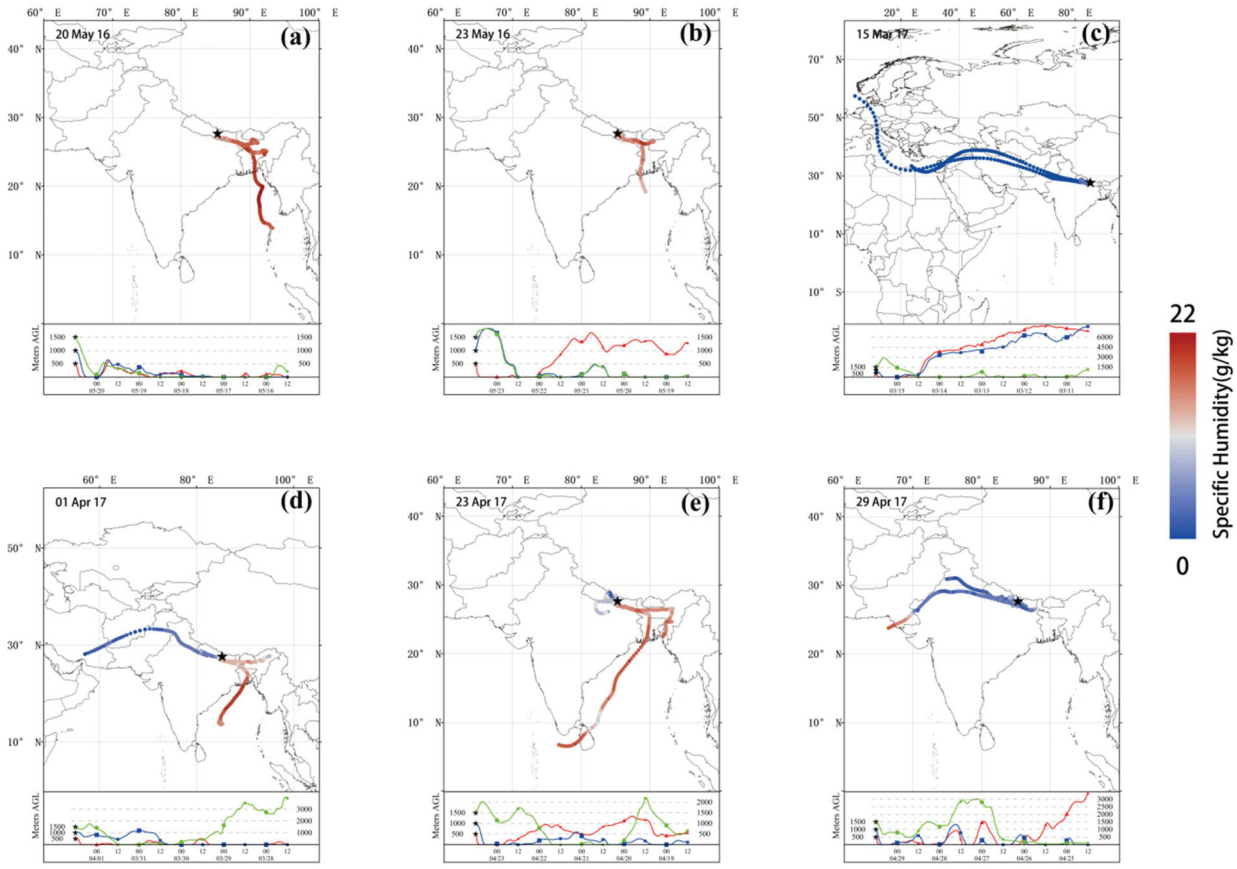

Fig. 7. Specific humidity variations along 5 d backward moisture trajectories calculated at 500 m, 1000 m, and 1500 m above ground level for precipitation events of Kathmandu on (a) 20 May 2016, (b) 23 May 2016, (c) 15 March 2017, (d) 01 April 2017, (e) 23 April 2017, and (f) 29 April 2017. (To distinguish different atmospheric height, see supplemental material, Fig. S1).

in non-monsoon season, the dominant moisture source for precipitation at Kathmandu originates from the intense advection of southern branch of the westerlies (Figs. 6d and 6e) which is generally dry and is characterized by occasional rainfall associated with enriched $\delta^{18}O$ values in precipitation at Kathmandu.

The moisture transport processes before the onset of summer monsoon in 2017 were tested by using the HYSPLIT model at three different altitudes (500 m, 1000 m and 1500 m above ground level (AGL)) to confirm the conclusion we got above. In order to indicate the possible water vapour sources contribute to rain at Kathmandu, variation of specific humidity along the backward trajectories was also calculated combined with back trajectory. Figure 7 shows the results of 120 h air-mass backward trajectory analysis along with the specific humidity for some events before the onset of summer monsoon. (20 May 2016, 23 May 2016, 15 March 2017, 01 April 2017, 23 April 2017, and 29 April 2017). On 20 and 23 May 2016 (lowest d-excess value (−28.97‰) was recorded on 23 May 2016), the moisture for precipitation during that period was mainly transported by local convection and marine air mass originated from the Bay of Bengal with high specific humidity (Figs. 7a and 7b). During that day, precipitation amount was recorded as 21.5 mm. Similar analysis was performed for 15 March 2017, 01 April 2017, 23 April 2017, and 29 April 2017 (Figs. 7c, d, e, f). We found that the westerlies are the sole dominant moisture transport for precipitation on 15 March 2017 at different height levels (Fig. 7c) with both higher values of precipitation $\delta^{18}O$ and d-excess. The specific humidity along the trajectories was low and almost constant within the trajectories path. Precipitation on that day was recorded as 8.9 mm and d-excess value was 11.59‰. However, on 1 April, 2017, the transport signals of both continental air mass and marine air mass was detected (Fig. 7d), but the specific humidity along the trajectory originating from Bay of Bengal was higher over the oceanic region, and then decreased gradually towards the inland. The precipitation on that day was reached

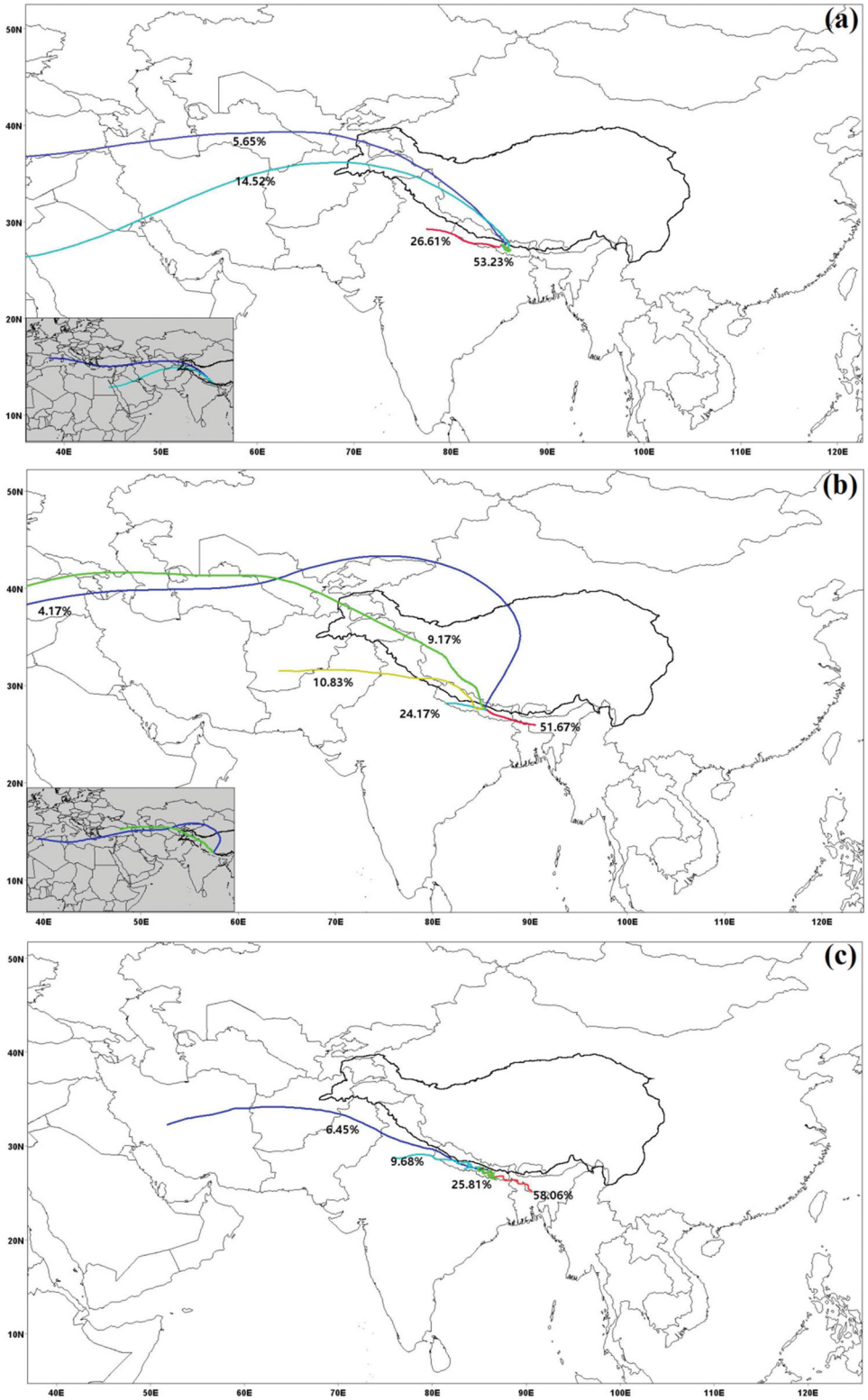

Fig. 8. Five days cluster-mean air parcel backward trajectories for (a) March, (b) April, and (c) May 2017. Dark black lines indicate the elevation higher than 3000 m asl.

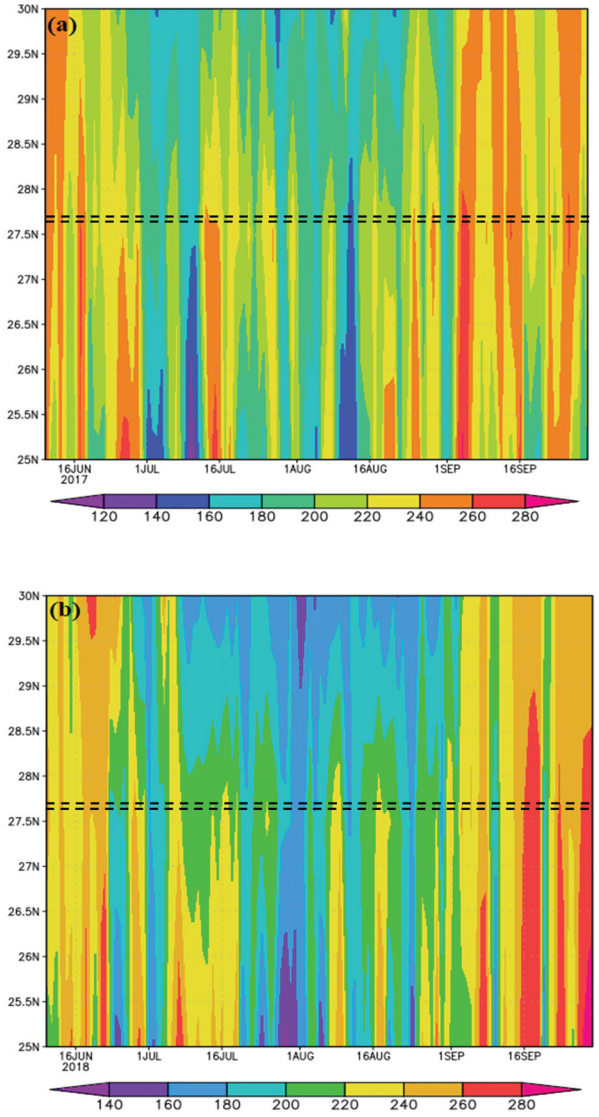

Fig. 9. Hovmöller diagram of OLR averaged over 84°E to 88°E during monsoon season of (a) 2017 and (b) 2018. The colour scale indicates OLR in W/m2. Dash parallel lines depict the latitudinal extends of sampling site.

from 3.2 mm (on 29 March 2017) to 12.6 mm and corresponding d-excess was varied from 9.50‰ (on 29 March 2017) to −18.30‰. On 23 April 2017, the influence of the westerlies is vanished instead of the local circulation, but strong transports from the Bay of Bengal are demonstrated (Fig. 7e). The decreasing or increasing of specific humidity along the trajectories indicated the possible contribution of precipitation or evaporation along the transport paths. On 29 April 2017, the moisture was mainly transported from the westerlies and marine air mass originated from Arabian Sea at different levels. The specific humidity along the trajectory was high in the region over Arabian Sea and quickly decreased over the land surface (Fig. 7f). On that day, the study site received precipitation amount of 10.6 mm and corresponding d-excess was −25.25‰.

Based on monthly clustering analysis in pre-monsoon season of 2017, we found Kathmandu mostly received moisture transported by the westerlies together with more than 50% of the local sources in March. (Fig. 8a), associated with enriched $\delta^{18}O$ and d-excess ($\delta^{18}O$ varied from 0.76‰ to 4.26‰ and d-excess varied from 3.65‰ to 19.54‰). In April, about 49% of moisture was transported from the westerlies and the local sources but larger percentage (about 51%) of moisture was transported from northeast India. (Fig. 8b). In May, about 58% of moisture was transported from northeast India close to Bay of Bengal together with 35% of local sources and only about 6% of moisture was contributed by the westerlies (Fig. 8c). Therefore, the polytropic precipitation stable isotopes at Kathmandu before the onset of summer monsoon reflect the combined effect of multiple moisture sources transported at different height levels. Hence, combined analysis of moisture backward trajectories and monthly clustering analysis showed that the interaction between different moisture sources produces complex variation in precipitation stable isotopes at Kathmandu before the onset of Indian monsoon. The extreme low d-excess values in some precipitation events before monsoon onset in 2016 and 2017 might be resulting from oceanic moisture sources with high humidity over the primary source region (Figs. 7b, d, f). This result is in agreement with some earlier studies (e.g. Jouzel et al., 2013; Klein et al., 2013; Benetti et al., 2014; Pfahl and Sodemann, 2014) which reported that the high ocean surface humidity results in the exceptionally depleted d-excess values.

3.6. Effect of convective activity on stable isotopes in precipitation

Recent studies have suggested that the variation of precipitation stable isotopes is related with convective activity along the moisture transport (Lekshmy et al. 2014; Permana et al., 2016; Saranya et al., 2018). We have identified the significant impact of moisture source and transport paths on precipitation stable isotopes at Kathmandu in above sections. Here we supposed the convective activity along the transport paths would vary the precipitation stable isotopes correspondingly. OLR is a useful indicator of deep tropical convective activity; and low OLR value reflects enhanced convection. Gadgil (2003) documented that OLR values less than 240 W/m^2 is indicative of large scale organized convection. The Hovmöller diagram of average OLR during monsoon period of 2017 (Fig. 9a) and 2018 (Fig. 9b) showed OLR values lower than 240 W/m^2 which indicated the presence of convective activity. The

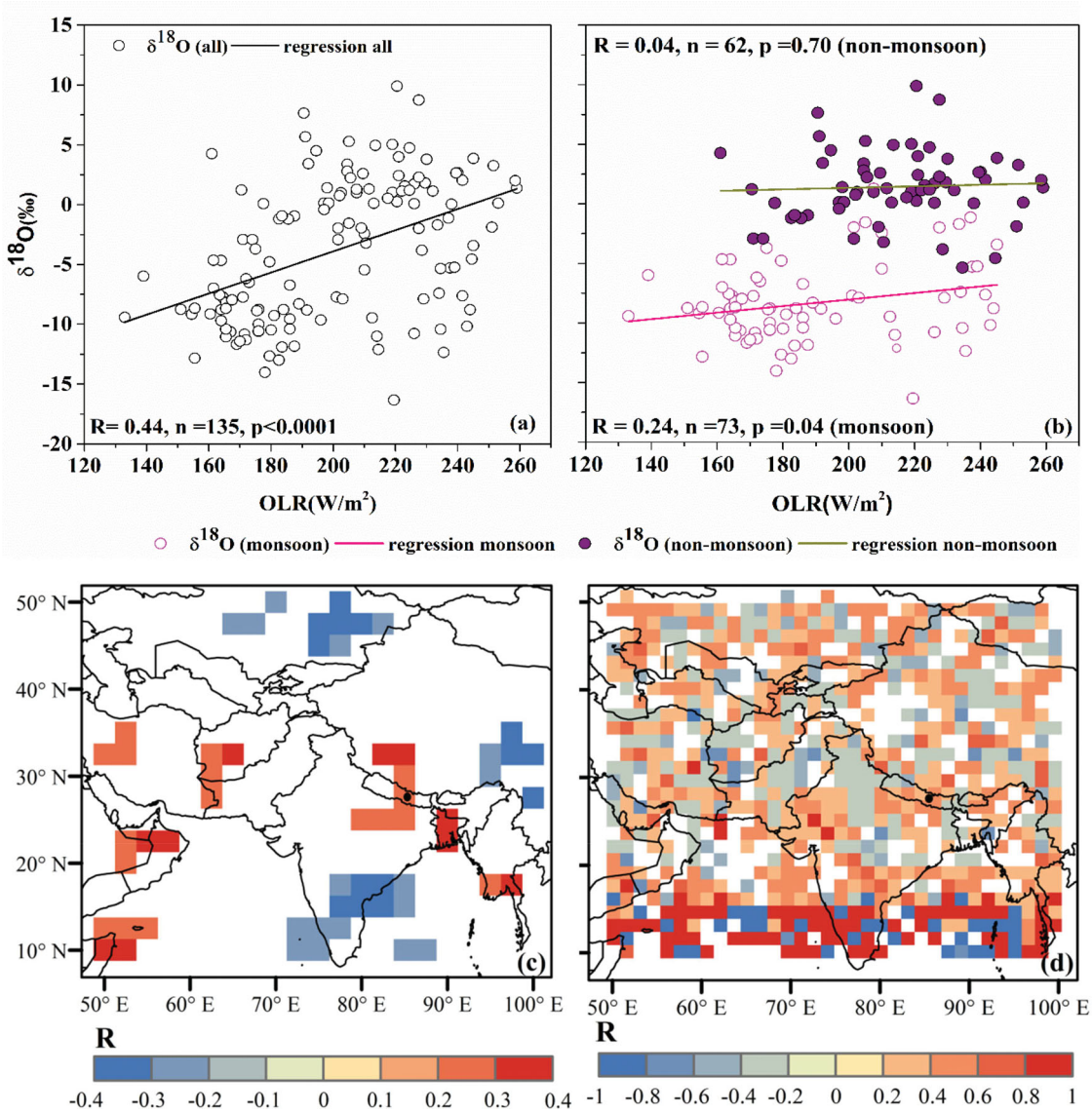

Fig. 10. Relation between $\delta^{18}O$ and OLR for (a) overall samples (b) during monsoon and non-monsoon period, (c) spatial correlation between $\delta^{18}O$ and OLR, and (d) spatial correlation between $\delta^{18}O$ and precipitation amount during monsoon season.

significant positive correlation was shown between $\delta^{18}O$ and daily mean OLR at sampling site ($R = 0.44$, $p < .0001$, $n = 135$) (Fig. 10a) and this relationship was continued in monsoon season ($R = 0.24$, $p < .05$, $n = 73$) but no significant correlation was found in non-monsoon season (Fig. 10b). Thus, we suggested that the significant impact of convective activity on precipitation stable isotopes exist in monsoon season. We calculated spatial correlation between precipitation $\delta^{18}O$ and OLR/precipitation amount in monsoon season (Fig. 10c and 10d). Our analysis shows that precipitation $\delta^{18}O$ at Kathmandu is positively correlated with OLR over Bangladesh, Myanmar, Northern India, central Nepal, some part of southern and central TP, and especially over the regions west to the Arabian Sea. These results agree with earlier studies (e.g. Gao et al., 2013; He et al., 2015), indicated the importance of regional convective activity in the variation of precipitation stable isotopes in monsoon season. Meanwhile negative correlation was observed over southeast TP, southern India, Kazakhstan and some parts of the Bay of Bengal and Arabian Sea (Fig. 10c). Precipitation $\delta^{18}O$ was positively correlated with precipitation amount in most of the regions over the Bay of Bengal and the Arabian Sea (Fig. 10b). The amount effect was captured over eastern Nepal, central and northern India and somewhat elongated towards a west direction. Hence, the correlation between precipitation $\delta^{18}O$ at Kathmandu and regional OLR captured the effect of convective activity in monsoon season, especially in the regions

where monsoon moisture was transported either from the Bay of Bengal or from the Arabian Sea (Fig. 10c). This implies the possible linkage between convection along the southeasterly and southwesterly moisture trajectories and depletion of precipitation $\delta^{18}O$ during monsoon season.

4. Conclusions

This study presents the daily and seasonal variations of precipitation stable isotopes at Kathmandu, Nepal situated in the south of Himalayas from 10 May 2016 to 21 September 2018. Precipitation $\delta^{18}O$ and δD showed low values in monsoon season and relatively high values in non-monsoon season. Significantly negative correlations were identified between daily $\delta^{18}O$ and both air temperature and precipitation but such correlation disappeared at seasonal scale. The amount effect was not significant during our sampling period. The positive correlation between OLR and $\delta^{18}O$ in monsoon season reflected the role of convective activity on variations of precipitation stable isotopes at Kathmandu. Results based on backward trajectory suggested that precipitation stable isotopes before the onset of summer monsoon are probably related with the mixing of multi-moisture combined with the westerlies transport. We concluded that the significant influence of moisture sources and convective activities on precipitation stable isotopes is identified even considering the classification of precipitation amount.

Acknowledgements

The authors thank the staffs from Kathmandu Centre for Research and Education (KCRE), CAS-TU, Nepal for collecting precipitation samples, and Department of Hydrology and Meteorology, government of Nepal for providing required meteorological data. Some data used in this paper are from NCEP/NCAR reanalysis I datasets (https://www.esrl.noaa.gov/psd/) and Global Data Assimilation System (GDAS) (ftp://arlftp.arlhq.noaa.gov/pub/archives/gdas0p5) to run HYSPLIT model Interface. TRMM_3B42 daily precipitation data was used to analyse the spatial correlation between precipitation amount and $\delta^{18}O$. In addition, authors would like to thank Mr. Sunil Subba for his continuous help and support during the study period.

Disclosure statement

No potential conflict of interest was reported by the author(s).

Funding

This work is jointly supported by Strategic Priority Research Program of Chinese Academy of Sciences (Grant No. 2019QZKK0208), Pan-Third pole Environment Study for a Green Silk Road (Pan-TPE) (Grant No. XDA20100000) and National Natural Science Foundation of China (Grant No. 41871068).

Supplementary material

Supplemental data for this article can be accessed here

References

Araguás-Araguás, L., Froehlich, K. and Rozanski, K. 1998. Stable isotope composition of precipitation over Southeast Asia. *J. Geophys. Res.* **103**, 28721–28742. doi:10.1029/98JD02582

Benetti, M., Reverdin, G., Pierre, C., Merlivat, L., Risi, C. and co-authors. 2014. Deuterium excess in marine water vapor: Dependency on relative humidity and surface wind speed during evaporation. *J. Geophys. Res. Atmos.* **119**, 584–593. doi:10.1002/2013JD020535

Bershaw, J., Penny, S. M. and Garzione, C. N. 2012. Stable isotopes of modern water across the Himalaya and eastern Tibetan plateau: Implications for estimates of paleoelevation and paleoclimate. *J. Geophys. Res. Atmos.* **117**, n/a–18. doi:10.1029/2011JD016132

Breitenbach, S. F. M., Adkins, J. F., Meyer, H., Marwan, N., Kumar, K. K. and co-authors. 2010. Strong influence of water vapor source dynamics on stable isotopes in precipitation observed in Southern Meghalaya, NE India. *Earth Planet. Sci. Lett.* **292**, 212–220. doi:10.1016/j.epsl.2010.01.038

Cai, Z. and Tian, L. 2016. Atmospheric controls on seasonal and interannual variations in the precipitation isotope in the East Asian Monsoon region. *J. Climate* **29**, 1339–1352. doi:10.1175/JCLI-D-15-0363.1

Chakraborty, S., Sinha, N., Chattopadhyay, R., Sengupta, S. and Mohan, P. M. and co-authors. 2016. Atmospheric controls on the precipitation isotopes over the Andaman Islands. *Bay of Bengal. Sci. Rep.* **6**, 1–11.

Chen, F., Zhang, M., Wang, S., Qiu, X. and Du, M. 2017. Environmental controls on stable isotopes of precipitation in Lanzhou, China: An enhanced network at city scale. *Sci. Total Environ.* **609**, 1013–1022. doi:10.1016/j.scitotenv.2017.07.216

Chhetri, T. B., Yao, T., Yu, W., Ding, L., Joswiak, D. and co-authors. 2014. Stable isotopic compositions of precipitation events from Kathmandu, southern slope of the Himalayas. *Chin. Sci. Bull.* **59**, 4838–4846. doi:10.1007/s11434-014-0547-4

Clark, I. and Fritz, P. 1997. The environmental isotopes. *Environ. Isot. Hydrogeol* 2.

Craig, H. 1961. Isotopic variations in meteoric waters. *Science.* **133**, 1702–1703. doi:10.1126/science.133.3465.1702

Crawford, J., Hollins, S. E., Meredith, K. T. and Hughes, C. E. 2017. Precipitation stable isotope variability and sub-cloud evaporation processes in a semi-arid region. *Hydrol. Process.* **31**, 20–34. doi:10.1002/hyp.10885

Dansgaard, W. 1964. Stable isotopes in precipitation. *Tellus.* **16**, 436–468.

Draxler, R. R. and Hess, G. D. 1998. An overview of the HYSPLIT_4 modelling system for trajectories. *Aust. Meteorol. Mag.* **47**, 295–308.

Froehlich, K., Gibson, J. J. and Aggarwal, P. K. 2001. Deuter*ium excess in precipitation and its climatological significance*. In: *Proceedings of Study of Environmental Change Using Isotope Techniques*, Vienna, IAEA, 54–66.

Gadgil, S. 2003. The Indian monsoon and its variability. *Annu. Rev. Earth Planet. Sci.* **31**, 429–467. doi:10.1146/annurev.earth.31.100901.141251

Gao, J., Masson-Delmotte, V., Yao, T., Tian, L., Risi, C. and co-authors. 2011. Precipitation water stable isotopes in the South Tibetan plateau: Observations and modeling. *J. Climate* **24**, 3161–3178. doi:10.1175/2010JCLI3736.1

Gao, J., Masson-Delmotte, V., Risi, C., He, Y. and Yao, T. 2013. What controls precipitation $\delta^{18}O$ in the southern Tibetan Plateau at seasonal and intra-seasonal scales? A case study at Lhasa and Nyalam. *Tellus B Chem. Phys. Meteorol.* **65**, 21043. doi:10.3402/tellusb.v65i0.21043

He, S. and Richards, K. 2016. Stable isotopes in monsoon precipitation and water vapour in Nagqu, Tibet, and their implications for monsoon moisture. *J. Hydrol.* **540**, 615–622. doi:10.1016/j.jhydrol.2016.06.046

He, Y., Risi, C., Gao, J., Masson-Delmotte, V., Yao, T. and co-authors. 2015. Impact of atmospheric convection on south Tibet summer precipitation isotopologue composition using a combination of in situ measurements, satellite data and atmospheric general circulation modeling. *J. Geophys. Res. Atmos.* **120**, 3852–3871. doi:10.1002/2014JD022180

Jouzel, J., Delaygue, G., Landais, A., Masson-Delmotte, V., Risi, C. and co-authors. 2013. Water isotopes as tools to document oceanic sources of precipitation. *Water Resour. Res.* **49**, 7469–7486. doi:10.1002/2013WR013508

Kalnay, E., Kanamitsu, M., Kistler, R., Collins, W., Deaven, D. and co-authors. 1996. The NCEP/NCAR 40-year reanalysis project. *Bull. Amer. Meteor. Soc.* **77**, 437–471. doi:10.1175/1520-0477(1996)077<0437:TNYRP>2.0.CO;2

Karki, R., Talchabhadel, R., Aalto, J. and Baidya, S. K. 2016. New climatic classification of Nepal. *Theor. Appl. Climatol.* **125**, 799–808. doi:10.1007/s00704-015-1549-0

Klein, E. S., Cherry, J. E., Young, J., Noone, D. and Leffler, A. J. and co-authors. 2013. Arctic cyclone water vapor isotopes support past sea ice retreat recorded in Greenland ice. *Nat. Publ. Gr* 1–9. Online at:.

Kleist, D. T., Parrish, D. F., Derber, J. C., Treadon, R., Wu, W.-S. and co-authors. 2009. Introduction of the GSI into the NCEP Global Data Assimilation System. *Wea. Forecasting* **24**, 1691–1705. doi:10.1175/2009WAF2222201.1

Lachniet, M. S. and Patterson, W. P. 2002. Stable isotope values of Costa Rican surface waters. *J. Hydrol.* **260**, 135–150. doi:10.1016/S0022-1694(01)00603-5

Lekshmy, P. R., Midhun, M., Ramesh, R. and Jani, R. A. 2014. 18O depletion in monsoon rain relates to large scale organized convection rather than the amount of rainfall. *Sci. Rep.* **4**, 1–5.

Liu, Z., Tian, L., Yao, T. and Yu, W. 2008. Seasonal deuterium excess in Nagqu precipitation: Influence of moisture transport and recycling in the middle of Tibetan Plateau. *Environ. Geol.* **55**, 1501–1506. doi:10.1007/s00254-007-1100-4

Munksgaard, N. C., Wurster, C. M., Bass, A. and Bird, M. I. 2012. Extreme short-term stable isotope variability revealed by continuous rainwater analysis. *Hydrol. Process.* **26**, 3630–3634. doi:10.1002/hyp.9505

Pang, Z., Kong, Y., Froehlich, K., Huang, T., Yuan, L. and co-authors. 2011. Processes affecting isotopes in precipitation of an arid region. *Tellus, Ser. B Chem. Phys. Meteorol.* **63**, 352–359. doi:10.1111/j.1600-0889.2011.00532.x

Pape, J. R., Banner, J. L., Mack, L. E., Musgrove, M. L. and Guilfoyle, A. 2010. Controls on oxygen isotope variability in precipitation and cave drip waters, central Texas, USA. *J. Hydrol.* **385**, 203–215. doi:10.1016/j.jhydrol.2010.02.021

Peng, H., Mayer, B., Harris, S. and Krouse, H. R. 2007. The influence of below-cloud secondary effects on the stable isotope composition of hydrogen and oxygen in precipitation at Calgary, Alberta, Canada. *Tellus B: Chem. Phys. Meteorol.* **59**, 698–704. doi:10.1111/j.1600-0889.2007.00291.x

Permana, D. S., Thompson, L. G. and Setyadi, G. 2016. Tropical West Pacific moisture dynamics and climate controls on rainfall isotopic ratios in southern Papua, Indonesia. *J. Geophys. Res. Atmos.* **121**, 2222–2245. doi:10.1002/2015JD023893

Pfahl, S. and Sodemann, H. 2014. What controls deuterium excess in global precipitation? *Clim. Past* **10**, 771–781. doi:10.5194/cp-10-771-2014

Ren, W., Yao, T. and Xie, S. 2017. Key drivers controlling the stable isotopes in precipitation on the leeward side of the central Himalayas. *Atmos. Res.* **189**, 134–140. doi:10.1016/j.atmosres.2017.01.020

Ren, W., Yao, T., Xie, S. and He, Y. 2016. Controls on the stable isotopes in precipitation and surface waters across the southeastern Tibetan Plateau. *J. Hydrol.* **545**, 276–287. doi:10.1016/j.jhydrol.2016.12.034

Risi, C., Bony, S. and Vimeux, F. 2008. Influence of convective processes on the isotopic composition (δ18O and δD) of precipitation and water vapor in the tropics: 2. Physical interpretation of the amount effect. *J. Geophys. Res.* **113**, 1–12.

Rozanski, K., Araguas-Araguas, L. and Gonfiantini, R. 1992. Relation between long-term trends of oxygen-18 isotope composition of precipitation and climate. *Science.* **258**, 981–985. doi:10.1126/science.258.5084.981

Rozanski, K., Araguás-Araguás, L. and Gonfiantini, R. 1993. Isotopic patterns in modern global precipitation. In: *Climate Change in Continental Isotopic Records. Geophysical Monograph* (eds. P. K. Swart, K. C. Lohmann, J. McKenzie,

S. Savin). Vol. 78, American Geo-Physical Union, Washington, DC, pp. 1–36.

Salamalikis, V., Argiriou, A. A. and Dotsika, E. 2016. Isotopic modeling of the sub-cloud evaporation effect in precipitation. *Sci. Total Environ.* **544**, 1059–1072. doi:10.1016/j.scitotenv.2015.11.072

Sánchez-Murillo, R., Esquivel-Hernández, G., Welsh, K., Brooks, E. S., Boll, J. and co-authors. 2013. Spatial and temporal variation of stable isotopes in precipitation across Costa Rica: an analysis of historic GNIP records. *Ojmh.* **03**, 226–240. doi:10.4236/ojmh.2013.34027

Saranya, P., Krishan, G., Rao, M. S., Kumar, S. and Kumar, B. 2018. Controls on water vapor isotopes over Roorkee, India: Impact of convective activities and depression systems. *J. Hydrol.* **557**, 679–687. doi:10.1016/j.jhydrol.2017.12.061

Shrestha, A. B., Wake, C. P., Dibb, J. E. and Mayewski, P. A. 2000. Precipitation fluctuations in the Nepal Himalaya and its vicinity and relationship with some large scale climatological parameters. *Int. J. Climatol.* **20**, 317–327. doi:10.1002/(SICI)1097-0088(20000315)20:3<317::AID-JOC476>3.0.CO;2-G

Tian, L., Masson-Delmotte, V., Stievenard, M., Yao, T. and Jouzel, J. 2001. Tibetan Plateau summer monsoon northward extent revealed by measurements of water stable isotopes. *J. Geophys. Res.* **106**, 28081–28088. doi:10.1029/2001JD900186

Wei, Z., Lee, X., Liu, Z., Seeboonruang, U., Koike, M. and co-authors. 2018. Influences of large-scale convection and moisture source on monthly precipitation isotope ratios observed in Thailand, Southeast Asia. *Earth Planet. Sci. Lett.* **488**, 181–192. doi:10.1016/j.epsl.2018.02.015

Wu, H., Zhang, X., Xiaoyan, L., Li, G. and Huang, Y. 2015. Seasonal variations of deuterium and oxygen-18 isotopes and their response to moisture source for precipitation events in the subtropical monsoon region. *Hydrol. Process.* **29**, 90–102. doi:10.1002/hyp.10132

Xie, L., Wei, G., Deng, W. and Zhao, X. 2011. Daily δ18O and δD of precipitations from 2007 to 2009 in Guangzhou, South China: Implications for changes of moisture sources. *J. Hydrol.* **400**, 477–489. doi:10.1016/j.jhydrol.2011.02.002

Yang, X., Yao, T., Yang, W., Yu, W. and Qu, D. 2011. Co-existence of temperature and amount effects on precipitation δ18O in the Asian monsoon region. *Geophys. Res. Lett.* **38**, n/a–6. doi:10.1029/2010GL045993

Yao, T., Thompson, L., Yang, W., Yu, W., Gao, Y. and co-authors. 2012. Different glacier status with atmospheric circulations in Tibetan Plateau and surroundings. *Nature Clim. Change* **2**, 663–667. doi:10.1038/nclimate1580

Yao, T., Masson-Delmotte, V., Gao, J., Yu, W., Yang, X. and co-authors. 2013. A review of climatic controls on δ18O in precipitation over the Tibetan Plateau: observation and simulations. *Rev. Geophys.* **51**, 525–548. doi:10.1002/rog.20023

Yao, T., Masson, V., Jouzel, J., Stievenard, M. Sun, W. and co-authors. 1999. Relationship between δ18O in precipitation and surface air temperature in the Urumqi river basin, east Tianshan mountains, China. *Geophys. Res. Lett.* **26**, 3473–3476.

Yu, W., Yao, T., Lewis, S., Tian, L., Ma, Y. and co-authors. 2014. Stable oxygen isotope differences between the areas to the north and south of Qinling Mountains in China reveal different moisture sources. *Int. J. Climatol.* **34**, 1760–1772. doi:10.1002/joc.3799

Yu, W., Yao, T., Tian, L., Ma, Y., Ichiyanagi, K. and co-authors. 2008. Relationships between δ18O in precipitation and air temperature and moisture origin on a south-north transect of the Tibetan Plateau. *Atmos. Res.* **87**, 158–169. doi:10.1016/j.atmosres.2007.08.004

Yu, W., Yao, T., Tian, L., Ma, Y., Wen, R. and co-authors. 2015. Short-term variability in the dates of the Indian monsoon onset and retreat on the southern and northern slopes of the central Himalayas as determined by precipitation stable isotopes. *Clim. Dyn.* **47**, 159–172. doi:10.1007/s00382-015-2829-1